

Ultrahigh-Field Hole Cyclotron Resonance Absorption in InMnAs Films

Y. H. Matsuda*

Department of Physics, Faculty of Science, Okayama University, 3-1-1 Tsushimanaka, Okayama 700-8530, Japan

G. A. Khodaparast, M. A. Zudov,[†] and J. Kono[‡]

Department of Electrical and Computer Engineering, Rice University, Houston, Texas 77005

Y. Sun, F. V. Kyrychenko, G. D. Sanders, and C. J. Stanton
Department of Physics, University of Florida, Gainesville, Florida 32611-8440

N. Miura, S. Ikeda, Y. Hashimoto, and S. Katsumoto
Institute for Solid State Physics, University of Tokyo, Kashiwa, Chiba 277-8581, Japan

H. Munekata

Image Science and Engineering Laboratory, Tokyo Institute of Technology, Yokohama, Kanagawa 226-8503
(Dated: June 18, 2018)

We have carried out an ultrahigh-field cyclotron resonance study of p -type $\text{In}_{1-x}\text{Mn}_x\text{As}$ films, with Mn composition x ranging from 0% to 2.5%, grown on GaAs by low-temperature molecular-beam epitaxy. Pulsed magnetic fields up to 500 T were used to make cyclotron resonance observable in these low-mobility samples. The clear observation of hole cyclotron resonance is direct evidence of the existence of a large number of itinerant, effective-mass-type holes rather than localized d -like holes. It further suggests that the p - d exchange mechanism is more favorable than the double exchange mechanism in this narrow gap InAs-based dilute magnetic semiconductor. In addition to the fundamental heavy-hole and light-hole cyclotron resonance absorption appearing near the high-magnetic-field quantum limit, we observed many inter-Landau-level absorption bands whose transition probabilities are strongly dependent on the sense of circular polarization of the incident light.

PACS numbers: 76.40.+b, 75.50.Pp, 71.18.+y, 07.55.Db

I. INTRODUCTION

The successful growth of Mn-based III-V dilute magnetic semiconductors (DMSs) by low temperature molecular beam epitaxy^{1,2,3,4,5} has opened up new device possibilities to make simultaneous use of magnetic and semiconducting properties. Although there exist different types of theoretical models to explain the microscopic mechanism of ferromagnetism in these semiconductors,^{6,7,8,9,10,11,12,13,14,15,16,17,18} a comprehensive picture has not been completed yet. Only an accepted fact at the present is that the ferromagnetic interaction between Mn ions is mediated by holes.

There are two limiting cases for the possible interaction mechanisms: the Ruderman-Kittel-Kasuya-Yosida (RKKY) type interaction⁶ and the double exchange (DE) type interaction.¹⁰ However, neither of them is likely to provide a complete explanation. The RKKY interaction is inconsistent with the fact that the estimated magnitude of the exchange interaction constant exceeds the Fermi energy as well as the fact that ferromagnetism occurs even in the insulating phase. On the other hand, the DE mechanism has the problem that the valence states of most of the Mn ions are found to be d^5 ($S = 5/2$); there has been no strong evidence that the d -holes which contribute to the DE interaction exist. Therefore, the real interaction mechanism may be described by another

model in which the character of the carrier is not pure p - or d -hole.

The Zener model, which is the limiting case of the RKKY model for small carrier concentrations, is one of the possible mechanisms.⁷ In this case, if the d state is deep enough in the valence band, holes at the Fermi level have almost p -type character since the anti-bonding state formed by the p - d hybridization is almost p -like and we can classify the system as a charge transfer insulator.⁷ However, there can be a case where the d -state is shallow and the holes have partly d -like character due to the strong p - d hybridization. When the itinerant holes are d -like, the reality is closer to the DE model.¹⁶ Therefore, investigating the degree of localization of holes is very important in clarifying the physical picture of the carrier-induced ferromagnetism.

Since cyclotron resonance (CR) directly provides the effective masses and scattering times of carriers, we can obtain detailed information on the itinerancy of the carriers. In DC transport measurements it is normally difficult to deduce the contributions of the mass and scattering time independently. Hence, CR on III-V ferromagnetic semiconductors is one of the most intriguing and urgently required experiments. However, since the mobilities of III-V ferromagnetic semiconductors are low ($< 100 \text{ cm}^2/\text{Vs}$), it is extremely difficult or impossible to observe CR in the magnetic field range of a conventional

superconducting magnet (< 20 T).

Recently, we reported results of an ultrahigh field (≤ 100 T) CR study of *electrons* in $\text{In}_{1-x}\text{Mn}_x\text{As}$ films.^{19,20} We described the dependence of cyclotron mass on x , ranging from 0 to 12%. We observed that the electron CR peak shifts to lower field with increasing x . Midinfrared interband absorption spectroscopy revealed no significant x dependence of the band gap. A detailed comparison of experimental results with calculations based on a modified Pidgeon-Brown model allowed us to estimate the s - d and p - d exchange constants α and β to be 0.5 eV and -1.0 eV, respectively.

In this paper we report the first observation of *hole* CR in p -type $\text{In}_{1-x}\text{Mn}_x\text{As}$ films using even higher magnetic fields (≤ 500 T). The observation of CR suggests that there are a large number of itinerant holes in InMnAs and they behave like effective mass carriers rather than d -like holes or holes tightly bound to the acceptor atoms. This suggests that Zener's p - d exchange interaction⁷ is more favorable as the ferromagnetic interaction mechanism than the DE interaction in InAs-based magnetic semiconductors.

The observation of CR is also consistent with the Drude-like behavior observed in the optical conductivity of InMnAs thin films reported recently.²¹ We also found that the observed CR mass is not very different from that of holes in InAs. We deduced the CR mobilities of several samples with different Mn concentrations from CR spectra at different photon energies and compared them with the values obtained by DC transport measurements.

Finally, we performed detailed theoretical calculations within the effective mass formalism using a modified Pidgeon and Brown model.^{20,22} We found that theoretical CR absorption spectra obtained by the simulations reproduce very well the complicated CR spectra at very high fields.

II. EXPERIMENTAL PROCEDURE

Since the mobility of a ferromagnetic III-V semiconductor is generally low (less than $100 \text{ cm}^2/\text{Vs}$), using ultrahigh magnetic fields exceeding 100 T (megagauss field) is essential for the present study in order to satisfy the CR condition $\omega_c\tau > 1$, where ω_c is the cyclotron frequency and τ is the scattering time.^{19,23} Two kinds of pulsed magnets are used for field generation: the single turn coil technique^{24,25} and the electromagnetic flux compression method.^{25,26} The single-turn coil method can generate 200 T without any sample damage and thus we can repeat measurements on the same sample under the same experimental conditions. For higher field experiments we use the electromagnetic flux compression method that can generate fields up to 600 T. This is a totally destructive method and we lose the sample as well as the magnet in each shot. The maximum energy stored in capacitor banks is 200 kJ for the single-turn coil method and 5 MJ for the electromagnetic flux compression method.

TABLE I: Characteristics of the $\text{In}_{1-x}\text{Mn}_x\text{As}$ samples used in the present work. All samples are $1 \mu\text{m}$ thick. The $x=0$ sample (InAs) is Be doped.

x	buffer	n_p (10^{19} cm^{-3})	μ (cm^2/Vs)	ρ ($\text{m}\Omega \text{ cm}$)	$T_c(\text{K})$
0	-	0.5	200	-	-
0.0015	-	1.1	59	6.6	-
0.003	-	2.30	56	4.9	< 4
0.0045	-	2.3	56	4.8	< 4
0.006	-	1.8	64	5.3	< 4
0.02	-	0.39	26	62	~ 4
0.025	InAs ^a	~ 1			< 10

^aThickness is 190 nm.

CR experiments were carried out by measuring the transmission of midinfrared radiation through the sample as a function of magnetic field. We use several types of infrared lasers as radiation sources. The wavelength range of the radiation was $28 \mu\text{m}$ to $3.39 \mu\text{m}$, corresponding to a photon energy range of 44 meV to 366 meV. The use of the high magnetic fields required these unusually high photon energies for CR. In addition, the photon energy had to be higher than the plasma frequency; the samples were heavily doped and the plasma frequency was estimated to be ~ 30 meV and ~ 60 meV for the light holes and heavy holes using effective masses of $0.026m_0$ and $0.35m_0$, respectively, and a concentration of $1 \times 10^{19} \text{ cm}^{-3}$.

We measured six p -InMnAs samples with various Mn concentrations ($x = 0, 0.003, 0.0045, 0.006, 0.02, \text{ and } 0.025$). The samples were grown by low temperature molecular beam epitaxy. The characteristics of the samples are shown in Table I. The hole concentration n_p , the mobility μ and the resistivity ρ shown were obtained by DC transport measurements at room temperature. The dimensions of the sample for the megagauss CR experiment were about $2 \times 2 \text{ mm}^2$ with $\sim 1 \mu\text{m}$ thickness. The thickness of the substrate (semi-insulating GaAs) was 0.5 mm. The temperature was controlled from room temperature to 10 K using a liquid-helium flow cryostat made of plastic.

III. EXPERIMENTAL RESULTS AND THEORETICAL ANALYSES

A. Mn Concentration Dependence

Typical room-temperature magneto-transmission spectra at $5.53 \mu\text{m}$ ($\hbar\omega = 0.224 \text{ eV}$) and $10.6 \mu\text{m}$ ($\hbar\omega = 0.117 \text{ eV}$) for different Mn concentrations are shown in Fig. 1. Quarter-wave plates were used to create a hole-active circularly polarized beam. For all samples, a broad absorption peak was observed at 80-100 T for $5.53 \mu\text{m}$ and at ~ 40 T for $10.6 \mu\text{m}$. Based on our detailed theoretical analysis (to be discussed later), we attribute

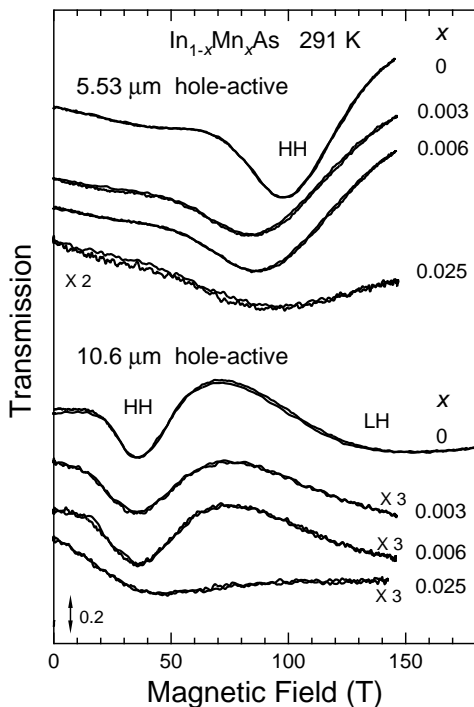


FIG. 1: Room temperature cyclotron resonance spectra for $\text{In}_{1-x}\text{Mn}_x\text{As}$ with various x taken with hole-active circularly-polarized $5.53 \mu\text{m}$ and $10.6 \mu\text{m}$ radiation.

this peak to heavy hole (HH) CR. We observe another absorption band at ~ 150 T with $10.6 \mu\text{m}$ radiation, and attribute it to light hole (LH) CR. The cyclotron masses and cyclotron mobilities of HH were deduced from the peak positions and widths, respectively, and plotted in Fig. 2. Only the transition between Landau levels with small indices (quantum numbers) contributes to the CR even at room temperature due to the large cyclotron energy at high fields in the megagauss range. Thus, the obtained masses are significantly smaller than the band edge HH mass ($0.35m_0$) due to the well known quantum effect in high magnetic fields.

As shown in Fig. 2(a), the HH cyclotron mass tends to decrease with x up to $x = 0.02$ when measured at $5.53 \mu\text{m}$. However, the HH mass for the $x = 0.025$ sample apparently deviates from this tendency. In addition, the HH mass obtained at $10.6 \mu\text{m}$ does not show any obvious dependence on the Mn concentration. It may suggest that some other effects such as strain and disorder are playing a role in determining the masses. Actually, as shown later, our detailed Landau level calculation at the high fields suggests that the HH band edge mass in $\text{In}_{1-x}\text{Mn}_x\text{As}$ is nearly the same with the HH band edge mass in InAs.

The cyclotron mobilities in Fig. 2(b) are larger than those obtained by DC transport measurements even in the nonmagnetic ($x = 0$) sample. This is partly because the HH cyclotron masses in this high field range are an

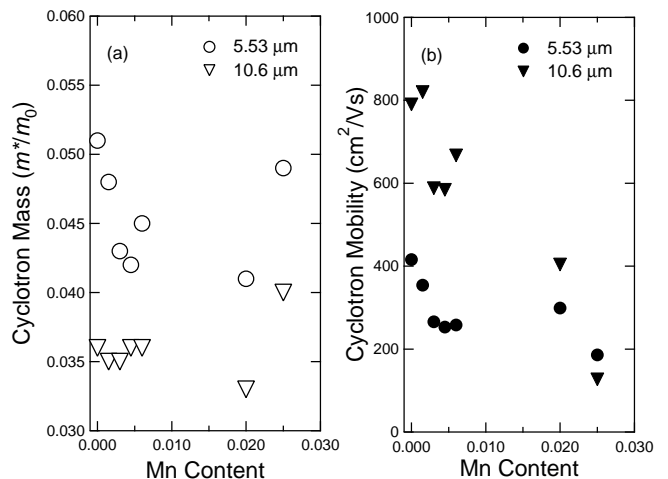


FIG. 2: Deduced cyclotron masses (a) and cyclotron mobilities (b) at 291 K as functions of Mn content, x . Open circles and open triangles shows cyclotron masses at $5.53 \mu\text{m}$ and $10.6 \mu\text{m}$, respectively. Closed circles and closed triangles denote the cyclotron mobilities at $5.53 \mu\text{m}$ and $10.6 \mu\text{m}$, respectively.

order of magnitude smaller than the classical value, as we pointed out above. Another possible origin of the discrepancy is the reduction of magnetic scattering at high fields, i.e., the randomness of Mn spins decreases at strong magnetic fields even at room temperature. This is consistent with the fact that the relative increase of the mobility compared to the DC value is larger for the magnetic samples than the nonmagnetic sample (InAs). However, the fact that cyclotron mobilities measured at $10.6 \mu\text{m}$ (resonance fields ~ 40 T) are larger than those measured at $5.53 \mu\text{m}$ (resonance field ~ 80 - 100 T) is not explainable by this picture. Since at room temperature the magnetization is not saturated even at 100 T, the randomness of Mn spins should be smaller for higher fields.²⁷ Although we take into account the mass increase due to the band non-parabolicity, the scattering time (τ) deduced from the cyclotron mass (m_{CR}) and the cyclotron mobility ($\mu^* = e\tau/m_{CR}$) is found to be smaller at $5.53 \mu\text{m}$ than that at $10.6 \mu\text{m}$. Moreover, the cyclotron mobility is not dependent on the temperature as we show later. Hence, it is expected that magnetic effects on scattering processes are suppressed at lower fields than the field range where we observed CR.

B. Temperature Dependence

CR spectra for the $x = 0.006$ and $x = 0.025$ samples at various temperatures are shown in Figs. 3(a) and 3(b), respectively. The HH CR peak position is found to be rather insensitive to the temperature in both samples, suggesting that any effect of temperature-dependent exchange splitting of the Landau levels is small. This is

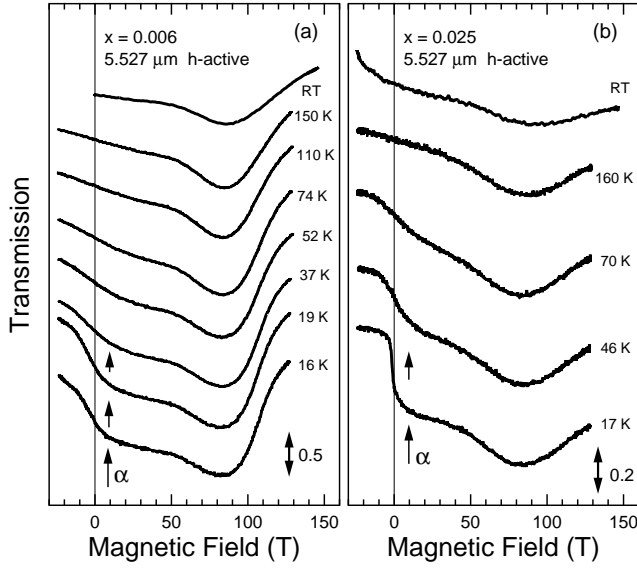


FIG. 3: Temperature-dependent cyclotron resonance traces for $\text{In}_{1-x}\text{Mn}_x\text{As}$ with (a) $x = 0.006$ and (b) $x = 0.025$. A new absorption band, labeled α , appears at low temperatures.

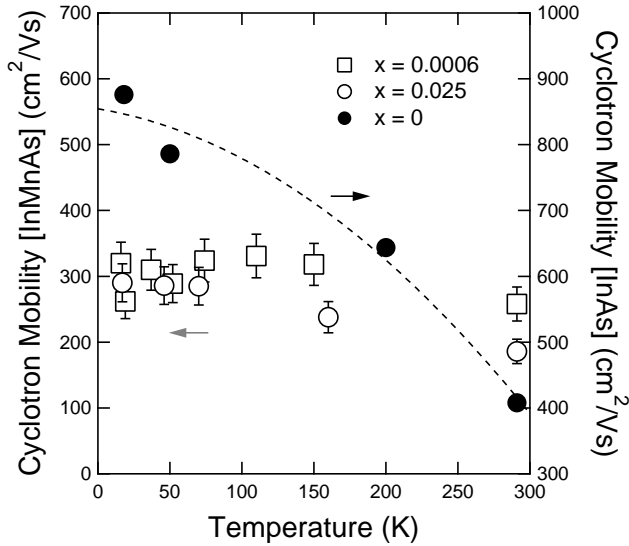


FIG. 4: Temperature dependence of cyclotron mobilities of heavy hole CR at $10.6 \mu\text{m}$ for $\text{In}_{1-x}\text{Mn}_x\text{As}$ ($x = 0, 0.006, 0.025$). Dashed curve is a guide for the eyes for the InAs data.

because the Mn concentration is small and the relative energy of the exchange splitting to the cyclotron energy is small in the megagauss range. Also, we find that the cyclotron mobility shows no significant change for both samples. This should be contrasted to the cyclotron mobility of InAs, which increases with decreasing temperature, as shown in Fig. 4. It is likely that impurity scatter-

ing is more significant in InMnAs than InAs and the effect of suppression of magnetic scattering at low temperature which is expected for InMnAs, is not large enough to be observed.

It should be noted that a new broad absorption band appears at low temperature and low fields below 20 T for both samples, Labeled ' α ' in Fig. 3. One of the possible origins of this band is impurity shifted CR (ICR) absorption. If this is the case, it could be closely related to the Mn impurity band and useful for clarifying the picture of ferromagnetism. However, our CR experiments at higher photon energies (see, e.g., the trace for $3.39 \mu\text{m}$ and 14 K in Fig. 5) and theoretical calculations indicate that this is not the case.

As we described previously,^{28,29} the width of the low field tail results from higher order Landau levels being populated and thus it depends on the free hole concentration. In addition, the sharpness of the low field cutoff is seen to depend on temperature and can be attributed to the sharpness of the Fermi distribution at low temperatures. The results show that the cyclotron resonance for the InMnAs case is made up of one strong heavy hole transition together with background absorption due to higher populated Landau levels at low values of the magnetic field. Hence, it is suggested that the electronic structure in $\text{In}_{1-x}\text{Mn}_x\text{As}$ is not strongly modified from that in InAs. Actually, our Landau level calculation using the Luttinger parameters for InAs can reproduce very well the CR absorption curves as shown later. (See Fig. 10.)

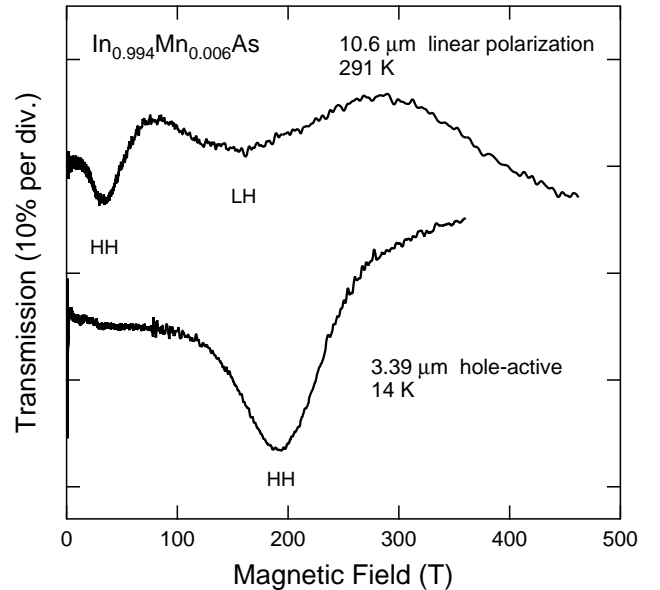


FIG. 5: Cyclotron resonance in $\text{In}_{1-x}\text{Mn}_x\text{As}$ ($x = 0.006$) at multi-megagauss fields. Only the HH CR is observed at $3.39 \mu\text{m}$ and 14 K. The absorption band observed at low fields and low temperatures for the wavelength of $5.53 \mu\text{m}$ (the band labeled α) is not observed.

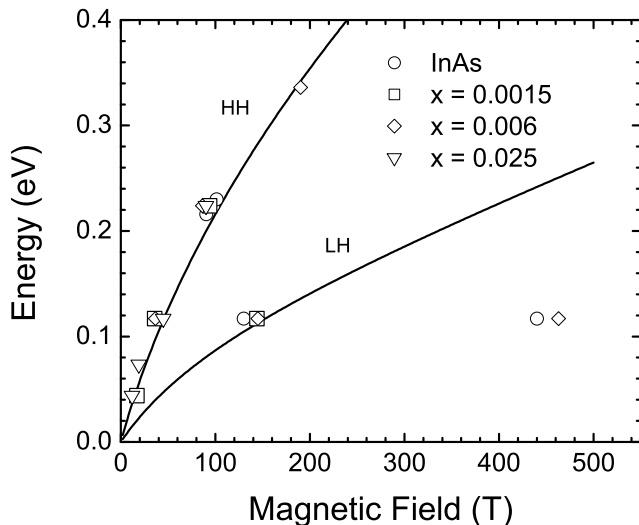


FIG. 6: Summary of the observed hole-active cyclotron resonance peak positions for four samples with different Mn contents. The solid curves are calculations based on an 8-band effective mass model for bulk InAs.

C. Photon Energy Dependence

Figure 6 summarizes the observed hole-active CR peak positions as a function of magnetic field (B). The solid curves show the calculated inter-Landau-level transitions for bulk InAs based on an 8-band Pidgeon-Brown model.^{19,20,28,30,31} The details of the calculations in terms of the effective mass theory is described in the next subsection. Although the effective mass theory could break down at such high fields since the magnetic length becomes $\sim 12 \text{ \AA}$ at 450 T, which is not too large compared to the lattice constant, we see that most of the CR transitions are explained well.

D. Landau Level Calculation

We have performed detailed calculations of the valence-band Landau levels within an 8-band $\mathbf{k}\cdot\mathbf{p}$, Pidgeon-Brown model^{20,22,30} including $sp-d$ coupling to the Mn ions to understand the observed CR. The Landau levels and the possible inter-Landau-level transitions are complicated at high fields due to wave function mixing.

Figure 7 shows the calculated Landau levels at the Γ point ($\mathbf{k} = 0$) as a function of magnetic field for $x = 0$ at 20 K. The Fermi energy corresponding to a hole concentration of $n_p = 1 \times 10^{19} \text{ cm}^{-3}$ is also indicated in the figure (dashed line). In the figure, we use the notation (n, m) to denote the levels. n corresponds to the manifold index ($n = -1, 0, 1, \dots$) and m denotes the state within the manifold (up to 8 states for manifolds $n = 2$ and higher). This notation is basically the same with the notation given by Pidgeon and Brown²² and discussed

in detail in the article by Kossut for narrow gap II-VI diluted magnetic semiconductors.³²

We used standard Luttinger parameters for InAs and took into account the $sp-d$ exchange interactions for calculations involving Mn doping. In this case, the exchange constants we used for the electron-Mn interaction (α) and hole-Mn ion (β) were 0.5 eV and -1.0 eV, respectively.¹⁹

Allowed optical transitions for h-active polarization and a laser energy of 0.117 eV, or wavelength of 10.6 μm (top curve in Fig. 5) are shown. Analysis of the wave functions for the first transition (≈ 50 T) show that this corresponds to a transition between the lowest and the second lowest spin down HH Landau levels (i.e., the dominant components of the wavefunctions are HH spin down). The next transition (≈ 150 T) occurs between the lowest and the second lowest spin down LH Landau levels. We thus label the experimental dips in the transmission (peaks in the absorption) HH and LH, respectively, in Figs. 5 and 7. We note that for low fields below 50 T, Fig. 7 shows absorption, though not any peak structure. This corresponds to transitions from

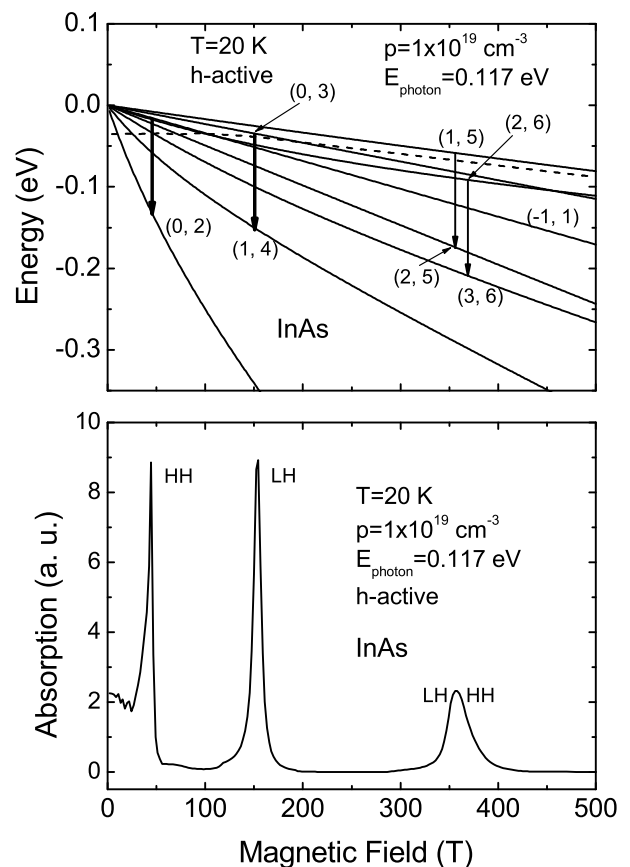


FIG. 7: Calculated Landau levels of the valence band at Γ point and CR absorption as functions of magnetic field for $x = 0$ at 20 K. The Fermi energy corresponding to the hole concentration $1 \times 10^{19} \text{ cm}^{-3}$ is also shown as the dashed line. The lower panel shows CR spectrum which corresponds to the inter-Landau level transitions shown in upper panel.

the many higher order Landau levels which lie below the Fermi energy at low magnetic fields. A similar feature is seen in the experimental data of Fig. 5.

At very high fields (> 300 T) the experimental data shows additional CR absorption (c.f. Fig. 5). This is also seen in the calculated CR absorption in Fig. 7. Our calculations show that this feature arises from multiple transitions, one being LH spin up like and the other being HH spin up like. While it appears that the (2,6) HH like transition lies below the Fermi level, the dominant part of this transition does not occur at $k = 0$. Figure 8 shows the E vs. k plot for $T = 20$ K and $B = 350$ T. As can be seen, the maximum of the (2,6) band occurs away from $k = 0$, and the $k = 0$ point is not occupied at a density of $p = 1 \times 10^{19} \text{ cm}^{-3}$. Our calculations show that the optical matrix element for the (2,6) \rightarrow (3,6) transition is strongest at the maximum point away from $k = 0$ and that for higher carrier densities, the CR absorption broadens to higher fields.

E. Electron-Active Hole Cyclotron Resonance

Hole CR can be observed not only with hole-active circularly polarized radiation but also with electron-active circularly polarized radiation due to the complex Landau level formation.³¹ Reversing the order of the Landau level index in the energy diagram for some Landau levels allows $N + 1 \rightarrow N$ type absorption transition that is active for the opposite circular polarization (electron active circular polarization) to the hole CR transition ($N \rightarrow N + 1$), where N denotes the Landau level index.

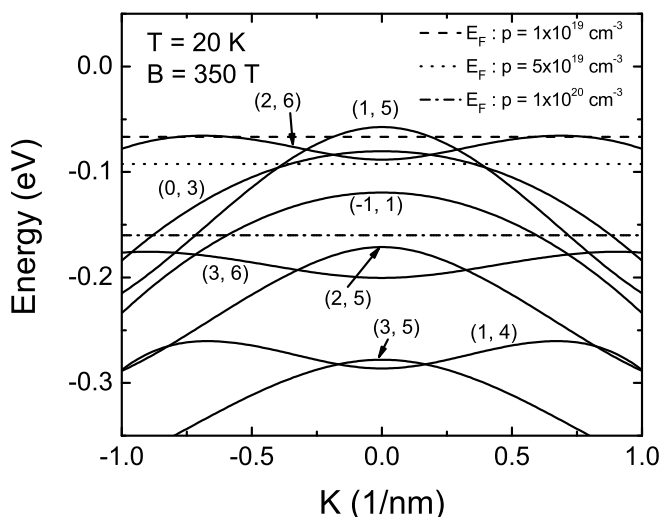


FIG. 8: Calculated energy E versus wavevector k (in the magnetic field direction) for $B = 350$ T. As can be seen, the maximum in the (2,6) Landau Level does not occur at $k = 0$. For higher carrier densities, the appropriate Fermi levels are shown. Higher carrier densities can lead to a much broader absorption feature.

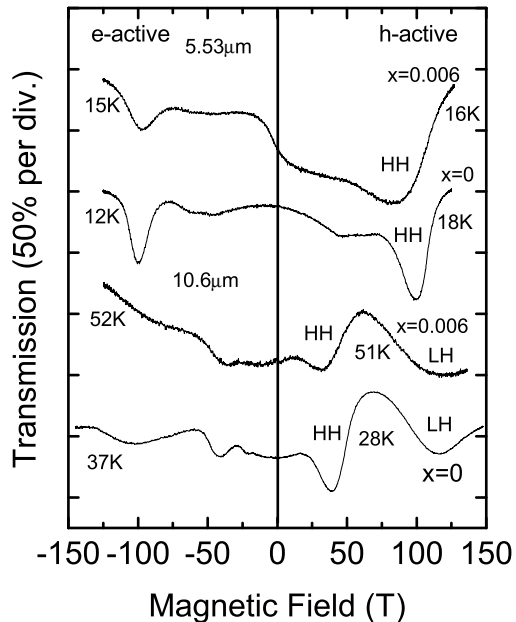


FIG. 9: Cyclotron resonance in $\text{In}_{1-x}\text{Mn}_x\text{As}$ ($x=0, 0.006$) at $10.6 \mu\text{m}$ (upper part of the figure) and at $5.53 \mu\text{m}$ (lower part of the figure). The right hand side of the figure corresponds to the results using the hole active circularly polarization of the radiation and the left hand side of the figure shows the results using the electron active circularly polarization.

In Fig. 9 electron active spectra are represented by reversing the sign of the magnetic field. Although the spectra look complicated, we can obtain rich information on the valence band parameters from the spectra. To understand details of the CR spectra, we have simulated the CR spectra using the Fermi's golden rule and the calculated Landau levels.

Figure 10 shows the result of the simulation and can be directly compared to Fig. 9. We see that the theory not only explains the CR peak positions but also the relative absorption intensity very well for both samples ($x = 0$ and $x = 0.006$). This fact suggests that the theoretical treatment, taken in this work, i.e., the effective mass theory and mean field approximation, is adequate for describing the electronic structure of the InAs-based DMS and the difference of the electronic structure between InAs and InMnAs is not very large when the Mn concentration is as small as 1%.

IV. CONCLUSIONS

Ultrahigh magnetic field cyclotron resonance experiments in p -type InMnAs thin films have revealed that not all of the holes are localized. The cyclotron resonance experiments are consistent with the delocalized holes with the effective masses given by the band structure ($0.35m_0$ for the heavy holes at the band edge). Our detailed theo-

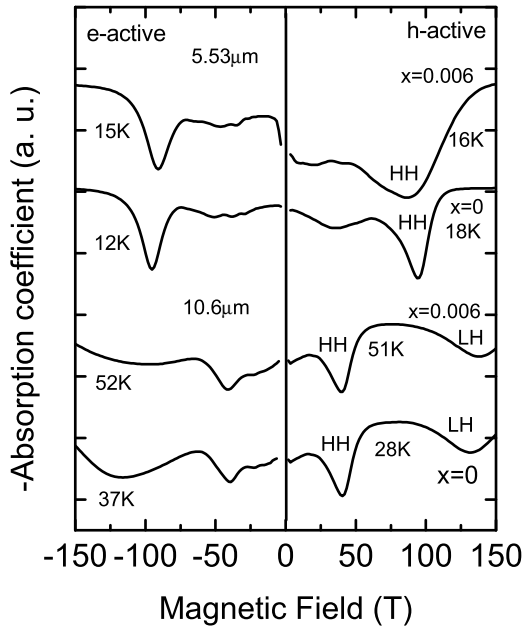


FIG. 10: Calculated CR spectra which can be directly compared to the experimental results shown in Fig. 9.

retical treatment using the effective mass theory within a mean field approximation for the polarization of the Mn ions successfully reproduced the complicated CR spectra. This fact strongly suggests that the mean-field approximation is adequate for the narrow gap InMnAs DMS and that the ferromagnetic transition can be understood in terms of Zener's $p-d$ exchange interaction rather than the double exchange interaction. Although the present experiments are only for $T > T_c$, recent experiments

in InMnAs/GaSb heterostructure samples below the ferromagnetic transition temperature²⁹ have confirmed the existence of delocalized holes in the ferromagnetic InMnAs DMS system.

We note, however, that hole CR has *not* been observed in ferromagnetic GaMnAs even in the megagauss range.^{27,33} Moreover, it has been reported that the optical conductivity spectrum shows non-Drude type behavior in GaMnAs^{34,35,36} while it clearly shows Drude type conductivity in InMnAs.²¹ These facts suggest that the hole character may be different in InMnAs and GaMnAs. According to the recent report on ZnCrTe,^{37,38} ferromagnetism can take place even if the conductive hole concentration is extremely low ($\sim 10^{15} \text{ cm}^{-3}$). Therefore, it is likely that the ferromagnetic transition mechanism is material dependent and strongly depends on the electronic states at the Fermi energy. We can imagine that the d -holes participate in the ferromagnetic transition mechanism in ZnCrTe and the nature of the hole states in GaMnAs falls between InMnAs and ZnCrTe.

We have shown that ultrahigh-field CR experiments are one of the most powerful methods to clarify the nature of carriers in the ferromagnetic semiconductors. It would be intriguing to perform CR experiments in a material with a moderate degree of localization between InMnAs and GaMnAs.

V. ACKNOWLEDGEMENTS

This work was supported by the NEDO International Joint Research Program and DARPA MDA972-00-1-0034 (SPINS), NSF DMR-0134058, NSF DMR-9817828, NSF INT-0221704.

* Electronic address: ymatsuda@cc.okayama-u.ac.jp

† Present address: Physics Department, University of Utah, Salt Lake City, Utah 84112.

‡ Electronic address: kono@rice.edu

¹ H. Munekata, H. Ohno, S. von Molnar, A. Segmuller, L. L. Chang, and L. Esaki, Phys. Rev. Lett. **63**, 1849 (1989).

² H. Munekata, H. Ohno, R. R. Ruf, R. J. Gambino, and L. L. Chang, J. Cryst. Growth **111**, 1011 (1991).

³ H. Ohno, H. Munekata, T. Penny, S. von Molnar, and L. L. Chang, Phys. Rev. Lett. **68**, 2664 (1992).

⁴ H. Munekata, A. Zaslavsky, P. Fumagalli, and R. J. Gambino, Appl. Phys. Lett. **63**, 2929 (1993).

⁵ H. Ohno, Science **281**, 951 (1998).

⁶ F. Matsukura, H. Ohno, A. Shen, and Y. Sugawara, Phys. Rev. B **57**, R2037 (1998).

⁷ T. Dietl, H. Ohno, and F. Matsukura, Phys. Rev. B **63**, 195205 (2001).

⁸ J. Konig, H. Lin, and A. H. MacDonald, Phys. Rev. Lett. **84**, 5628 (2000).

⁹ A. Chattopadhyay, S. D. Sarma, and A. J. Millis, Phys.

Rev. Lett. **87**, 227202 (2001).

¹⁰ H. Akai, Phys. Rev. Lett. **81**, 3002 (1998).

¹¹ J. Inoue, S. Nonoyama, and H. Itoh, Phys. Rev. Lett. **85**, 4610 (2000).

¹² V. I. Litvinov and V. K. Dugaev, Phys. Rev. Lett. **86**, 5593 (2001).

¹³ M. Berciu and R. N. Bhatt, Phys. Rev. Lett. **87**, 107203 (2001).

¹⁴ M. Takahashi and K. Kubo, Phys. Rev. B **66**, 153202 (2002).

¹⁵ M. Shirai, Physica E **10**, 143 (2001).

¹⁶ H. Katayama-Yoshida and K. Sato, Physica B **327**, 337 (2003).

¹⁷ Y. Zhao, W. Geng, K. T. Park, and A. J. Freeman, Phys. Rev. B **64**, 035207 (2001).

¹⁸ M. Jain, L. Kronik, J. R. Chelikowsky, and V. V. Godlevski, Phys. Rev. B **64**, 245205 (2001).

¹⁹ M. A. Zudov, J. Kono, Y. H. Matsuda, T. Ikaida, N. Miura, H. Munekata, G. D. Sanders, Y. Sun, and C. J. Stanton, Phys. Rev. B **66**, 161307 (2002).

- ²⁰ G. D. Snaders, Y. Sun, F. V. Kyrychenko, C. J. Stanton, G. A. Khodaparast, J. Kono, Y. H. Matsuda, N. Miura, T. Slupinski, A. Oiwa, et al., *Phys. Rev. B* **68**, 165202 (2003).
- ²¹ K. Hirakawa, A. Oiwa, and H. Miunekata, *Physica E* **10**, 215 (2001).
- ²² C. R. Pidgeon and R. N. Brown, *Phys. Rev.* **146**, 575 (1966).
- ²³ Y. H. Matsuda, T. Ikaida, N. Miura, S. Kuroda, F. Takano, and K. Takita, *Phys. Rev. B* **65**, 115202 (2002).
- ²⁴ K. Nakao, F. Herlach, T. Goto, S. Takeyama, T. Sakakibara, and N. Miura, *J. Phys. E* **18**, 1018 (1985).
- ²⁵ N. Miura, Y. H. Matsuda, K. Uchida, S. Todo, T. Goto, H. Mitamura, T. Osada, and E. Ohmichi, *Physica B* **294-295**, 562 (2001).
- ²⁶ Y. H. Matsuda, F. Herlach, S. Ikeda, and N. Miura, *Rev. Sci. Instrum.* **73**, 4288 (2002).
- ²⁷ Y. H. Matsuda, H. Arimoto, N. Miura, A. Twardowski, H. Ohno, A. Shen, and F. Matsukura, *Physica B* **256-258**, 565 (1998).
- ²⁸ G. D. Snaders, Y. Sun, C. J. Stanton, G. A. Khodaparast, J. Kono, Y. H. Matsuda, N. Miura, T. Slupinski, A. Oiwa, and H. Munekata, *J. Appl. Phys.* **93**, 6897 (2003).
- ²⁹ G. A. Khodaparast, M. Zudov, J. Kono, Y. H. Matsuda, T. Ikaida, S. Ikeda, N. Miura, T. Slupinski, A. Oiwa, H. Munekata, et al., *J. Supercond.* **16**, 107 (2003).
- ³⁰ G. D. Sanders, Y. Sun, C. J. Stanton, G. A. Khodaparest, J. Kono, Y. H. Matsuda, N. Miura, T. Slupinski, A. Oiwa, and H. Munekata, *Journ. of Superconductivity* **16**, 449 (2003).
- ³¹ Y. Sun, G. D. Sanders, F. V. Kyrychenko, C. J. Stanton, G. A. Khodaparest, J. Kono, Y. H. Matsuda, N. Miura, and H. Munekata, *Physica E* **20**, 374 (2004).
- ³² J. Kossut, *Semiconductors and Semimetals* **25**, 183 (1988).
- ³³ Y. H. Matsuda, H. Arimoto, N. Miura, H. Ohno, A. Shen, and F. Matsukura, *Ext. Abstract of the 3rd Symposium on the Phys. and Appl. of Spin-Related Phenomena in Semicond., Sendai, Japan* (1997).
- ³⁴ E. J. Singley, R. Kawakami, D. Awschalom, and D. N. Basov, *Phys. Rev. Lett.* **89**, 097203 (2002).
- ³⁵ K. Hirakawa, S. Katsumoto, T. Hayashi, Y. Hashimoto, and Y. Iye, *Phys. Rev. B* **65**, 193312 (2002).
- ³⁶ Y. Nagai, T. Kunimoto, K. Nagasaka, H. Nojiri, M. Motokawa, F. Matsukura, T. Dietl, and H. Ohno, *Jpn. J. Appl. Phys.* **40**, 6231 (2001).
- ³⁷ H. Saito, V. Zayets, S. Yamagata, and K. Ando, *Phys. Rev. B* **66**, 081201 (2002).
- ³⁸ H. Saito, V. Zayets, S. Yamagata, and K. Ando, *Phys. Rev. Lett.* **90**, 207202 (2003).